

g  
D-90

JOINT INSTITUTE FOR NUCLEAR RESEARCH

Laboratory of Nuclear Problems

P - 273(eng)

A.F. Dunaitzev, Yu.D. Prokoshkin

REACTION  $p + p \rightarrow p + p + \pi^0$  IN THE ENERGY RANGE

FROM THE THRESHOLD TO 665 MEV

*MC 77, 1959, t 36, 66, c 1656-1674.*

Dubna, 1959.

A.F. Dunaitzev, Yu.D. Prokoshkin

REACTION  $p + p \rightarrow p + p + \pi^0$  IN THE ENERGY RANGE  
FROM THE THRESHOLD TO 665 MEV\*)

Объединенный институт  
ядерных исследований  
БИБЛИОТЕКА

Dubna, 1959.

---

\*) The results of this investigation were reported at the 4-th Session of the Scientific Council of JINR in May 1958.

### A b s t r a c t

The angular distribution of  $\pi^0$  mesons produced in proton-proton collisions have been investigated at 400-665 Mev. The distributions were found to be close to isotropic in agreement with the phenomenological resonance theory of S. Mandelstam. The total cross sections were measured in the energy range 313-665 Mev. At energies above 400 Mev the main contribution to the reaction cross section is given by the resonant transitions. At the lower proton energies the non-resonant Ss-transition becomes essential, its contribution to the total cross section being  $0.032 \eta_m^2 \cdot 10^{-27} \text{ cm}^2$ . The comparison of the measured cross sections for neutral and charge pion production with those calculated from the resonance theory makes it possible to conclude that the transitions with the total angular momentum  $J = 2$  becomes preferential.

\* \* \*

## I. Introduction

The reaction of  $\pi^0$  meson production in proton-proton collisions occupies a special place among the reactions of the "nucleon + nucleon  $\rightarrow$   $\pi$  meson" type. Its characteristic feature is the rapid increase of the cross section with energy and a comparatively small value of the cross section near the threshold. This is the consequence of prohibition of the transition in final state: S for nucleons and p for  $\pi$  meson with respect to the center of mass, playing the main role in other reactions of meson production (Sp-transition in Rosenfeld's classification<sup>1/</sup>). The first investigations of this reaction<sup>2-8/</sup> showed that in the energy region 340 - 480 Mev its cross section  $\sigma_{pp}^{\pi^0}$  increases as  $\eta_m^8$  where  $\eta_m$  is the maximum momentum of  $\pi^0$  meson in the center of mass system (c.m.s.), measured in units of meson mass  $m_{\pi}c$ , while for the cross sections of other reactions the dependence upon  $\eta_m$  in the power of no higher than 4 is characteristic. Phenomenological analysis of these data<sup>1,9/</sup> showed that near the threshold the reaction (1) is fulfilled due to Pp-transition. In papers<sup>10,6,II/</sup> published later it was established that the cross section  $\sigma_{pp}^{\pi^0}$  keeps on increasing rapidly at energies 450 - 660 Mev also:  $\sigma_{pp}^{\pi^0} \sim \eta_m^{4.5}$  according to Soroko's data<sup>6/</sup> and  $\sigma_{pp}^{\pi^0} \sim \eta_m^{5.5}$  according to<sup>II/</sup>. Comparison of the data<sup>7,8,II/</sup> showed that in the low energy region the cross section changes rather as  $\eta_m^6$  than as  $\eta_m^8$ . From this the conclusion was drawn<sup>II/</sup> of the essential role of Ss-transition at low energies. The further investigations of the reaction (I) cross section at low energies<sup>12/</sup> confirmed this conclusion.

The experimental data obtained in<sup>II/</sup> were analysed by Mandelshtam on the basis of the phenomenological resonance theory<sup>13/</sup>. In difference to the former phenomenological theory<sup>I,9/</sup> Mandelshtam takes into account the resonant interaction of  $\pi$  meson with nucleon in the final state. His theory suggests that in the wide energy region where the resonant meson-nucleon interaction is of importance, the matrix transition elements are constant except for the factors taking account of meson-nucleon and nucleon-nucleon interaction in final state. The theory takes into account nucleon states interference and "displaced" transitions<sup>7/</sup>. S state production when one of nucleon is in S state with respect to meson-nucleon subsystem for which the only  $^2P_{3/2}$  state is taken, is described by one parameter and P state production by five parameters. The theory

turned out to be non-critical to the relative change of P state production parameters. This permitted to equal some of them to each other and thus to reduce a number of P state production parameters obtained experimentally from five to two. All three parameters describing S and P state production are determined from the experimental data on the reactions of charged  $\pi$  meson production in pp collisions. Total cross sections for the reaction (I) are calculated from Mandelshtam's theory with no introduction of any additional free parameters. Due to this fact the comparison of the experimental data on the energy dependence of this cross section with the theoretical curve is a good test of the resonant theory. The corresponding comparison with data of<sup>II/</sup> made by Mandelshtam showed that the experimental and theoretical data are in a good agreement.

The angular distribution of  $\pi^0$  mesons in the reaction (I) calculated from the resonant theory is close to isotropic at all the proton energies. Experiments performed by different methods at the energy about 600 Mev<sup>II,14,16/</sup> indicate that the angular distribution of  $\pi^0$  mesons are isotropic. However, at lower energies (450-550Mev) the measured angular distributions had the tendency to increasing the anisotropy<sup>II/</sup>. In the region of lower energies the angular distribution was analysed by Moyer and Squire<sup>17/</sup> with the definite assumptions on the  $\pi^0$  meson spectrum character, based on the former phenomenological theory<sup>I,9/</sup>. On the basis of the above assumptions they concluded that the angular distribution of  $\pi^0$  mesons at 330 Mev is essentially anisotropic.

The aim of the present work was to investigate the reaction (I) in a wide energy region. The using of the same methods permitted to hope to obtain rather accurate data on changing the characteristic of the reaction with energy. The main attention was drawn to the little known characteristic of the reaction, i.e., the angular distribution of  $\pi^0$  mesons. In making such investigations it is necessary to take into account the difficulty arising due to the fact that  $\pi^0$  mesons move with the velocity which essentially differs from the velocity of light. Because of this the angular distribution of  $\gamma$  rays produced in  $\pi^0$  meson decay is to the less degree anisotropic than that of  $\pi^0$  mesons<sup>18/</sup>. The anisotropy of  $\gamma$  ray angular distribution disappears rapidly with decreasing the  $\pi^0$  meson velocity (Fig.I). Here the event is considered when  $\pi^0$  mesons are distributed in c.m.s. proportionally to  $1/3 + b_{\pi^0} \cos^2 \vartheta$ . In this case the angular distribution of  $\gamma$  rays has the form  $1/3 + b_{\gamma} \cos^2 \vartheta$ . Fig. I gives value  $db_{\pi^0}/db_{\gamma}$  that is the measurement error of  $b_{\pi^0}$  at different energies of protons  $E_p$  producing  $\pi^0$  mesons. It is seen that the error increases rapidly with

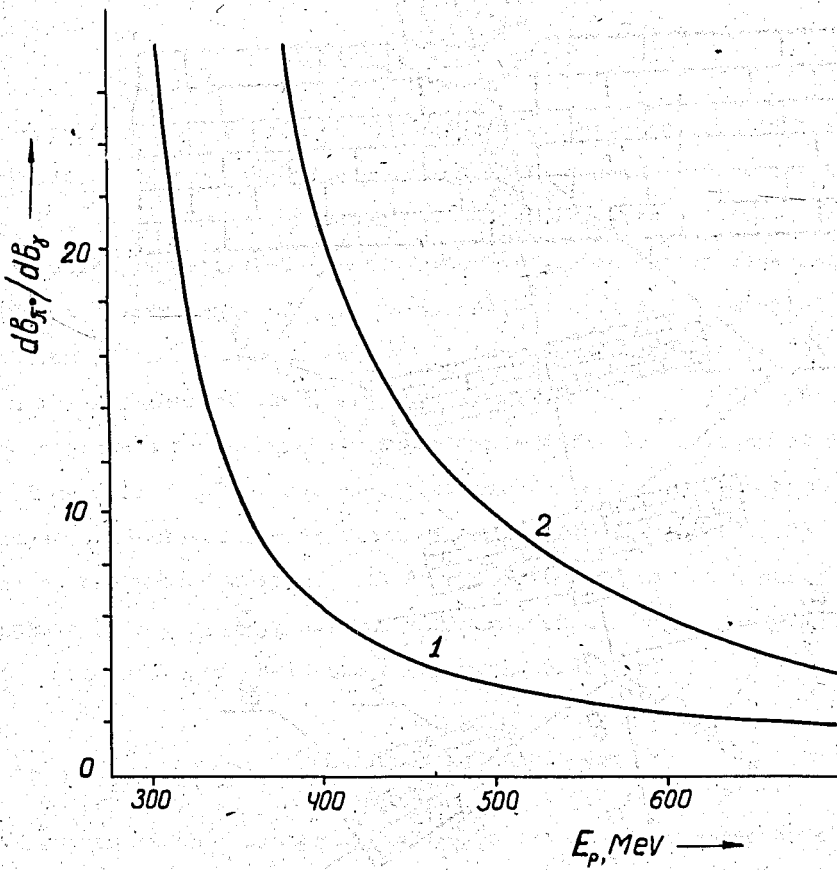


Fig. 1. Dependence of the relative error  $db_x/db_f$  upon proton energy. 1. - calculated for the cases  $b_x \approx 0$ , 2 - for  $b_x = 1$ .

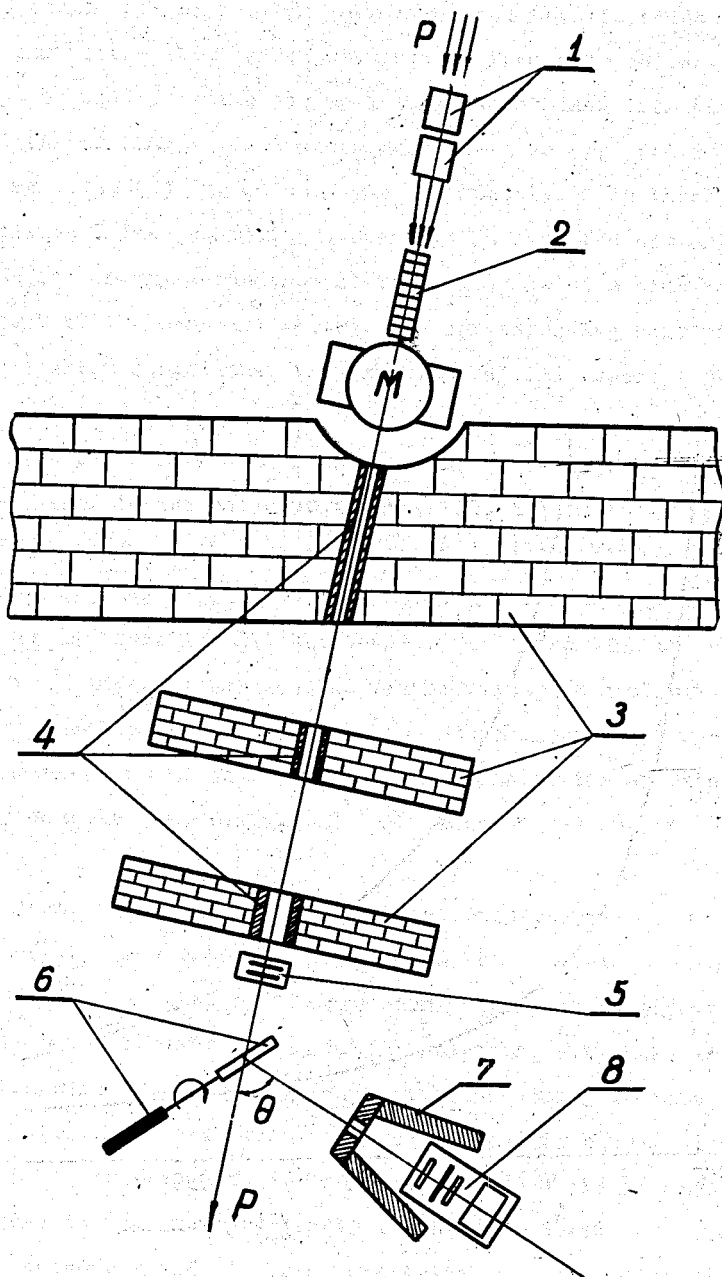


Fig. 2. Experimental arrangement (arbitrary scale).  
1. Focusing magnetic lens. 2. Polyethelene absorber. 3. Shielding. 4. Steel collimators. 5. Ionization chamber. 6. Targets. 7. A part of  $\gamma$ -telescope lead shielding. 8.  $\gamma$ -telescope. M. Deflecting magnet. P. Proton beam.

decreasing  $E_p$  and so increases the accuracy of  $\gamma$  ray angular distribution measurement necessary for reconstructing the angular distribution of  $\pi^0$  mesons. It should be taken into account also that in decreasing the proton energy together with increasing the demands to measurement accuracy the yield of  $\gamma$  rays emitted in the reaction under investigation rapidly decreases. This makes the measurement of  $\pi^0$  meson angular distributions even more complicated. In the present investigation we have measured the angular distributions of  $\gamma$  rays in the energy region 400-665 Mev where the difficulties indicated above were not so great and the equipment used permitted rather accurately to obtain the angular distribution of  $\pi^0$  mesons.

## 2. Experimental Methods

### Proton beam

The experiments were made on the unpolarized external proton beam of the 6 meter synchrocyclotron of the JINR. The beam intensity was measured with the accuracy of 3% by means of a calibrated ionization chamber filled with helium. As the cross section for the reaction investigated depends upon the proton energy especially near the threshold the measurements of the cross sections must be accompanied by the accurate determination of the beam mean energy. At low proton energies it is necessary to make precision measurements of the energy spectrum of a beam as well. The mean energy of the beam was determined in the present experiments with the accuracy of about 1 Mev by the method described in<sup>19/</sup>. The energy of protons was decreased by slowing them down in polyethelene blocks placed in front of the shielding wall (Fig.2). The energy distribution of the proton beam is well described by the Gaussian curve with the dispersion equal to  $(2.8 \pm 0.3)$  Mev at the maximum proton energy. As is seen from Fig.3 the dispersion somewhat increases with slowing the beam down.

### Registering equipment

Information of the angular distribution of  $\pi^0$  mesons and on the total cross sections were obtained by registering  $\gamma$  rays emitted in the decay of  $\pi^0$  mesons produced on the target bombarded by the proton beam. To detect  $\gamma$  rays a telescope consisted of counters was used (Fig.4). Gamma-rays produced on the target were collimated by means of a lead diaphragm and fall on the lead converter where they generated electron-positron pairs. The pairs were registered by coincidence scintillation and Čerenkov counters. Due to a small thickness of the converter (0.5 - 2 mm) and scintillators (3mm), "wide geometry" of the telescope and the lack of filters



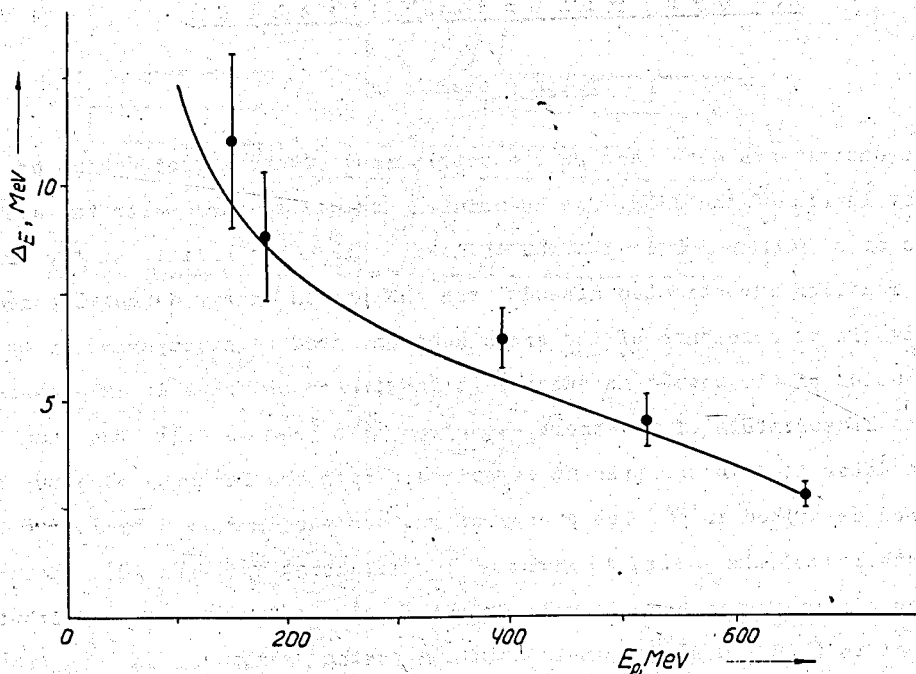


Fig. 3. Dispersion of a beam  $\Delta E$  at different proton energies  $E_p$  <sup>19/</sup>. The solid curve represents the theoretical energy dependence calculated by taking into account the increase of the ionization loss and the dispersion of the "straggling" type.

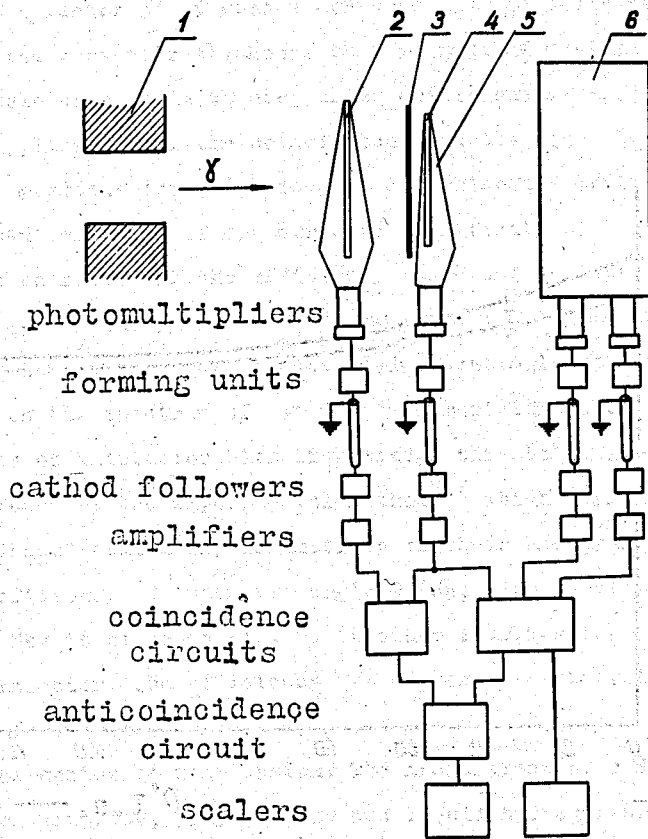


Fig. 4. Diagram of  $\gamma$ -telescope.  
1. Lead diaphragm. 2. Crystal of the anticoincidence counter. 3. Converter.  
4. Crystal of the coincidence counter. 5. Foil-reflector. 6. Radiator of Čerenkov counter.

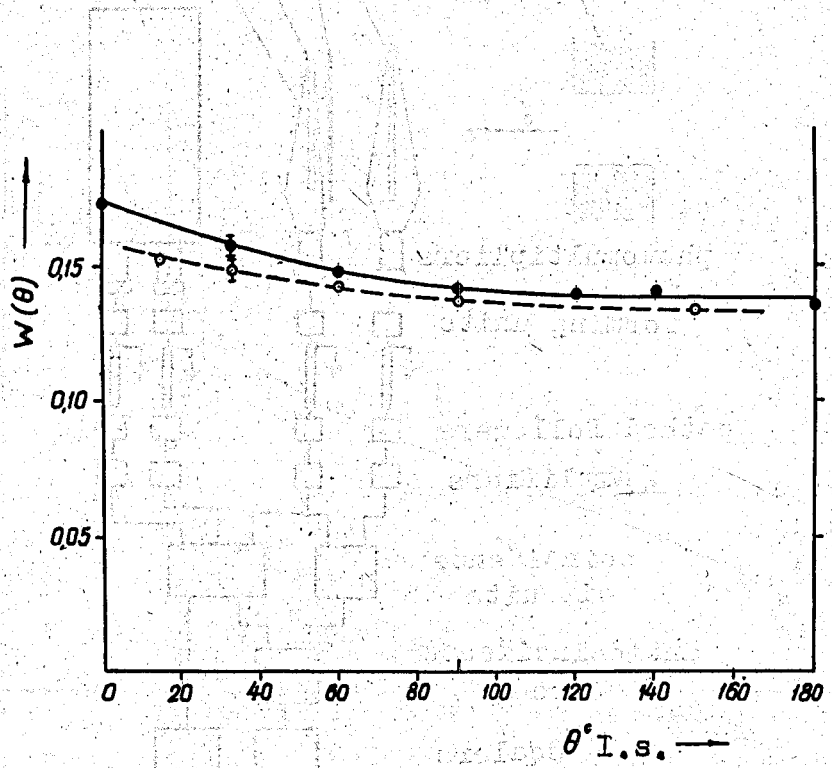


Fig. 5.  $\gamma$ -telescope efficiency  $W$ .

- -measured at  $E = 665$  Mev.
- -measured at  $E = 485$  Mev.

between counters,  $\gamma$ -telescope had a low energy threshold and could effectively detect  $\gamma$  rays of the energy up to 10 Mev. The telescope was sensitive neither to neutrons nor to charged particles. The latter was achieved by using a scintillation counter placed in front of the converter and set in anticoincidence with the other telescope counters. The counting rate of the telescope placed in the path of  $\gamma$  rays increased by a factor of 25 when a converter 2 mm thick was inserted into it. The increase of the converter thickness to 5 mm made it possible to improve this ratio up to 40. The telescope could be used under conditions of a comparatively large background due to the application of the coincidence circuits with the resolving time  $10^{-8}$  sec.

In most previous investigations to determine the efficiency of  $\gamma$ -telescope the measurement was made of the curve of sensitivity of  $\gamma$ -telescope to  $\gamma$ -rays of different energies and the efficiency was found by integrating this curve over the energy together with a spectra of  $\gamma$  rays taken from the theory. Therefore, the results obtained in these investigations depended essentially upon the validity of theoretical assumptions on the spectrum of  $\gamma$ -rays, especially in cases<sup>6,17/</sup> when measurements were made by means of a detector with high energy threshold. In the present paper the efficiency was found by the experimental method<sup>11/</sup> which permitted to find the yield of  $\gamma$  rays without making any assumptions on their energy spectrum. Dependence of the telescope efficiency  $W$  upon the angle  $\theta$  (see Fig. 2) measured at proton energies 665 and 485 Mev is given in Fig. 5. At other energies the dependence  $W(\theta)$  has the analogous character. The efficiency  $W$  decreases with proton energy and simultaneously changes the form of the curve  $W(\theta)$  due to decrease of  $\pi^+$  meson energy and the velocity of the center of mass system. The measurement of efficiency  $W(\theta)$  carried out at 665 Mev on graphite, polyethelene and liquid hydrogen targets showed that the value  $W$  for hydrogen and carbon coincide. This is due to the fact that the  $\gamma$ -telescope has low energy threshold. In spite of the sharp difference in  $\gamma$  ray spectra at  $\theta = 0^\circ$  and  $\theta = 180^\circ$ <sup>(20)</sup> (mean energies of the spectra are equal to 190 and 75 Mev), the efficiency  $W(0^\circ)$  and  $W(180^\circ)$  differ only as much as 25%.<sup>\*</sup> Much less difference is observed in the spectra measured for carbon and hydrogen at the same angle<sup>16,20/</sup>. Because of this the corresponding efficiencies are very close to each other. The difference in efficiency for hydrogen and carbon somewhat increases with decreasing proton energy. However in the investigated energy region this difference has no effect on the results of the measurements performed, as it was considerably less than the statistical accuracy of measurements of  $\gamma$  ray yield ratios at different angles.

between counters,  $\gamma$ -telescope had a low energy threshold and could effectively detect  $\gamma$  rays of the energy up to 10 Mev. The telescope was sensitive neither to neutrons nor to charged particles. The latter was achieved by using a scintillation counter placed in front of the converter and set in anticoincidence with the other telescope counters. The counting rate of the telescope placed in the path of  $\gamma$  rays increased by a factor of 25 when a converter 2 mm thick was inserted into it. The increase of the converter thickness to 5 mm made it possible to improve this ratio up to 40. The telescope could be used under conditions of a comparatively large background due to the application of the coincidence circuits with the resolving time  $10^{-8}$  sec.

In most previous investigations to determine the efficiency of  $\gamma$ -telescope the measurement was made of the curve of sensitivity of  $\gamma$ -telescope to  $\gamma$ -rays of different energies and the efficiency was found by integrating this curve over the energy together with a spectra of  $\gamma$  rays taken from the theory. Therefore, the results obtained in these investigations depended essentially upon the validity of theoretical assumptions on the spectrum of  $\gamma$  rays, especially in cases<sup>6,17/</sup> when measurements were made by means of a detector with high energy threshold. In the present paper the efficiency was found by the experimental method<sup>II/</sup> which permitted to find the yield of  $\gamma$  rays without making any assumptions on their energy spectrum. Dependence of the telescope efficiency  $W$  upon the angle  $\theta$  (see Fig. 2) measured at proton energies 665 and 485 Mev is given in Fig. 5. At other energies the dependence  $W(\theta)$  has the analogous character. The efficiency  $W$  decreases with proton energy and simultaneously changes the form of the curve  $W(\theta)$  due to decrease of  $\pi^0$  meson energy and the velocity of the center of mass system. The measurement of efficiency  $W(\theta)$  carried out at 665 Mev on graphite, polyethelene and liquid hydrogen targets showed that the value  $W$  for hydrogen and carbon coincide. This is due to the fact that the  $\gamma$ -telescope has low energy threshold. In spite of the sharp difference in  $\gamma$  ray spectra at  $\theta = 0^\circ$  and  $\theta = 180^\circ$ <sup>(20)</sup> (mean energies of the spectra are equal to 190 and 75 Mev), the efficiency  $W(0^\circ)$  and  $W(180^\circ)$  differ only as much as 25%.<sup>\*</sup> Much less difference is observed in the spectra measured for carbon and hydrogen at the same angle<sup>16,20/</sup>. Because of this the corresponding efficiencies are very close to each other. The difference in efficiency for hydrogen and carbon somewhat increases with decreasing proton energy. However in the investigated energy region this difference has no effect on the results of the measurements performed, as it was considerably less than the statistical accuracy of measurements of  $\gamma$  ray yield ratios at different angles.

The latter made it possible to use functions  $W(\theta)$  measured for carbon in obtaining the angular distribution of  $\gamma$  rays from the reaction (I) in the low energy region of protons.

#### Targets. Control experiments

As a target a liquid hydrogen was used poured into a styrofoam container. The target was of a cylindrical form 8 cm in diameter, 25 cm long and was placed so that the beam passing along the cylinder axis should not fall on the side walls of the target (the beam width was 6 cm). The registration conditions were most favorable in the angular region  $45^\circ < \theta < 145^\circ$ . In this case the lead diaphragm placed in front of the telescope prevented the  $\gamma$  radiation passing from the outlet and inlet target windows, from coming into the telescope. Thus, the telescope detected  $\gamma$  radiation emitted from hydrogen only. The counting rate of the telescope at 660 Mev decreased by a factor of 10 when hydrogen was removed from the container.

The cross section for the reaction (I) was determined also by the subtraction method. For this the polyethelene and graphite targets were exposed to the beam. The targets thickness equalled about  $3\text{g/cm}^2$  and was taken so that the energy loss of beam in the target was the same. Polyethelene and graphite targets were placed at  $45^\circ$  to the proton beam, as is shown in Fig.2 and were put into the beam in turn. The targets were changed in 1 - 3 min ; this permitted to avoid the effect arising due to the change in sensitivity of the registering equipment upon the measurement accuracy. In spite of the fact that polyethelene contain only 14% of hydrogen-in some case the subtraction method permitted to obtain much higher accuracy than it was in a case when a liquid hydrogen target was used. The reason of this is in the difficulty of the precision determination of the effective volume of the liquid hydrogen target in which  $\gamma$  rays registered by the telescope are produced. Therefore the liquid hydrogen was usually used for making precision relative measurements, absolute measurements being performed by the subtraction method.

To obtain rather high counting rate the telescope was placed at a small distance from the target. Here  $\gamma$  radiation emitted from different points of the target was detected by the telescope with different efficiency, the latter depending upon the target dimensions. We shall denote further the above efficiency determined by the target dimensions a formfactor of a target. The graphite target was made of light

graphite of  $0.9 \text{ g/cm}^3$  density; due to this formfactors of polyethelene and graphite targets differed only slightly. The maximum difference of formfactors for the targets used was 1.5% at  $\theta = 90^\circ$ ; this value rapidly decreased with decreasing the angle  $\theta$ . Since the ratios of  $\gamma$  ray yields from the target were to be measured with the accuracy up to 1%, a great attention was paid to the problem of determining the target formfactors. The formfactors were determind experimentally at different angles  $\theta$  with the accuracy better than 0.5%. A number of control experiments carried out with targets of different forms showed a good agreement between measured and calculated formfactors. The main and the most complicated control experiment was made at the proton energy 275 Mev. As this energy value lies below the threshold of the reaction of  $\pi^0$  meson production in pp collisions the ratio of cross sections for hydrogen and carbon measured by subtraction method must be equal to zero if the formfactors are found correctly. The value close to zero was really found from the experiment:

$$(\sigma_{pp}^r / \sigma_{pc}^r)_{\text{measured}} = -0.001 \pm 0.006$$

### 3. Results

#### Angular distributions of $\gamma$ rays

In the proton high energy region the investigations of angular distributions of  $\gamma$  rays were carried out both by the subtraction method and by using liquid hydrogen. In the first case the measurements were carried out in two stages: the measurement was made of the angular distribution of  $\gamma$  rays produced in collisions of protons with carbon nuclei  $f_{pc}^r(\vartheta)$  and then for each observation angle there was found the ratio of differential cross sections for hydrogen and carbon  $\sigma_{pp}^r = (d\sigma_{pp}^r/d\Omega) / (d\sigma_{pc}^r/d\Omega)$ . The angular distribution of  $\gamma$  rays produced on carbon by protons with the energy  $E = 665 \text{ Mev}^*$ ) is given in Fig.6. The angular distributions  $f_{pc}^r(\vartheta)$  at low energies have the analogous form. The measurement of relative cross section values  $\sigma_{pp}^r$  was made by the subtraction method at energies  $E = 665, 560$

---

\*/ Here and further E denotes the effective beam energy, determined by taking into account the energy loss in a target and the dispersion of a beam.

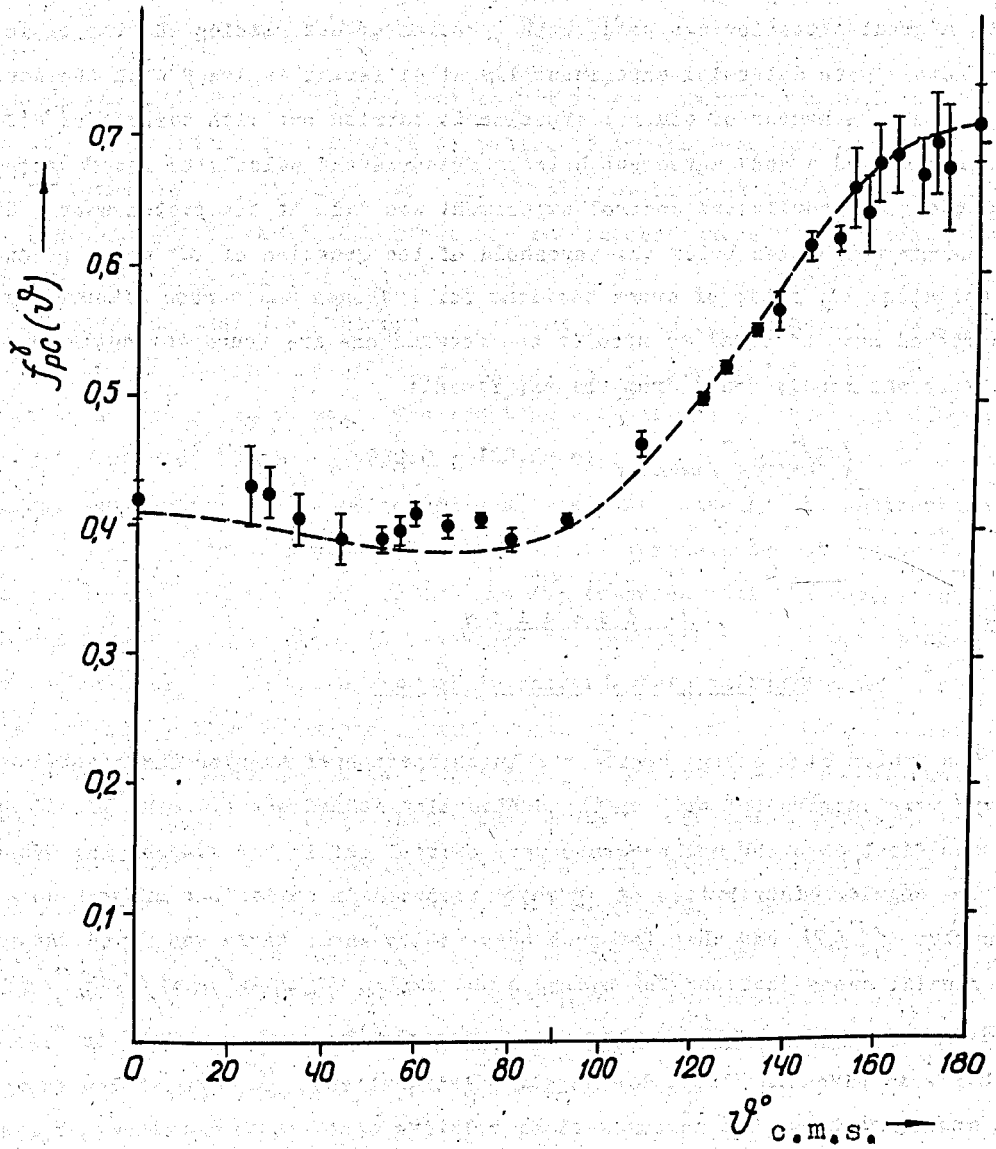


Fig. 6. Angular distribution of  $\gamma$  rays produced on carbon by 665 Mev protons. The curve is calculated on the basis of the optical model<sup>15/</sup>.



and 485 Mev for a great number of values  $\theta$  (see tables I,II,III).

T a b l e I E = 665 Mev

$\theta^\circ$	16	20	33	45	60	75	96	120	135	145	160
$\epsilon'_{pp}, \%$	14.7±0.8	15.4±0.8	14.9±0.5	14.5±0.8	12.7±0.6	11.6±0.8	10.8±0.5	9.9±0.4	9.2±0.8	9.4±1.2	10.0±1.2

T a b l e II E = 560 Mev

$\theta^\circ$	16	34	60	90	130	150
$\epsilon'_{pp}, \%$	9.9 ± 0.6	9.4 ± 0.9	7.5 ± 0.7	6.8 ± 0.5	6.4 ± 1.0	6.0 ± 0.7

T a b l e III E = 485 Mev

$\theta^\circ$	16	35	60	90	130	150
$\epsilon'_{pp}, \%$	5.1 ± 1.0	5.3 ± 0.5	5.6 ± 0.8	4.4 ± 0.7	4.0 ± 0.7	4.5 ± 0.9

So detailed an investigation of the function  $f_{pp}^{\gamma}(\vartheta)$  was made in order to check if there are systematic errors in the used measurement method. The distribution of  $\gamma$  rays produced in pp collisions must be symmetrical about the angle  $\vartheta = 90^\circ$  in the o.m. system as the colliding particles are indistinguishable. Therefore every deviation in the measured distribution from symmetry should be considered to be an indication to the presence of systematic errors in the method. The angular distribution of  $\gamma$  rays at E = 665 Mev obtained from the data of Fig.6. and Table I is given in Fig. 7. It is described by polynomial  $f_{pp}^{\gamma}(\vartheta) \sim 1/3 + (0.07 \pm 0.02)\text{Cos}^2\vartheta$ . This function found by the least square method and respectively normalized is shown in Fig. 7. The angular distribution of  $\gamma$  rays obtained turned out to be symmetrical. If approximating it by a polynomial which together with zero and the second terms contains also an asymmetrical term proportional to  $\text{Cos}\vartheta$ , its contribution will be negligible:  $(0.009 \pm 0.011)\text{Cos}\vartheta$ . The analysis of the measured distribution  $f_{pp}^{\gamma}(\vartheta)$  shows also that the contribution of the cosine powers higher than 2 is negligible; the fraction of  $\gamma$  rays distributed as  $\text{Cos}^4\vartheta$  is only  $(0.015 \pm 0.030)$ . This must take place at lower proton energies also, since the role of the states with greater momenta decreases towards the reaction threshold. Therefore it is possible to suggest that in the energy region  $E \leq 660$  Mev the angular distribution of  $\gamma$  rays from the reaction (I) has the form:

$$f_{pp}^{\gamma}(\vartheta) \sim 1/3 + b_{\gamma}\text{Cos}^2\vartheta. \quad (2)$$

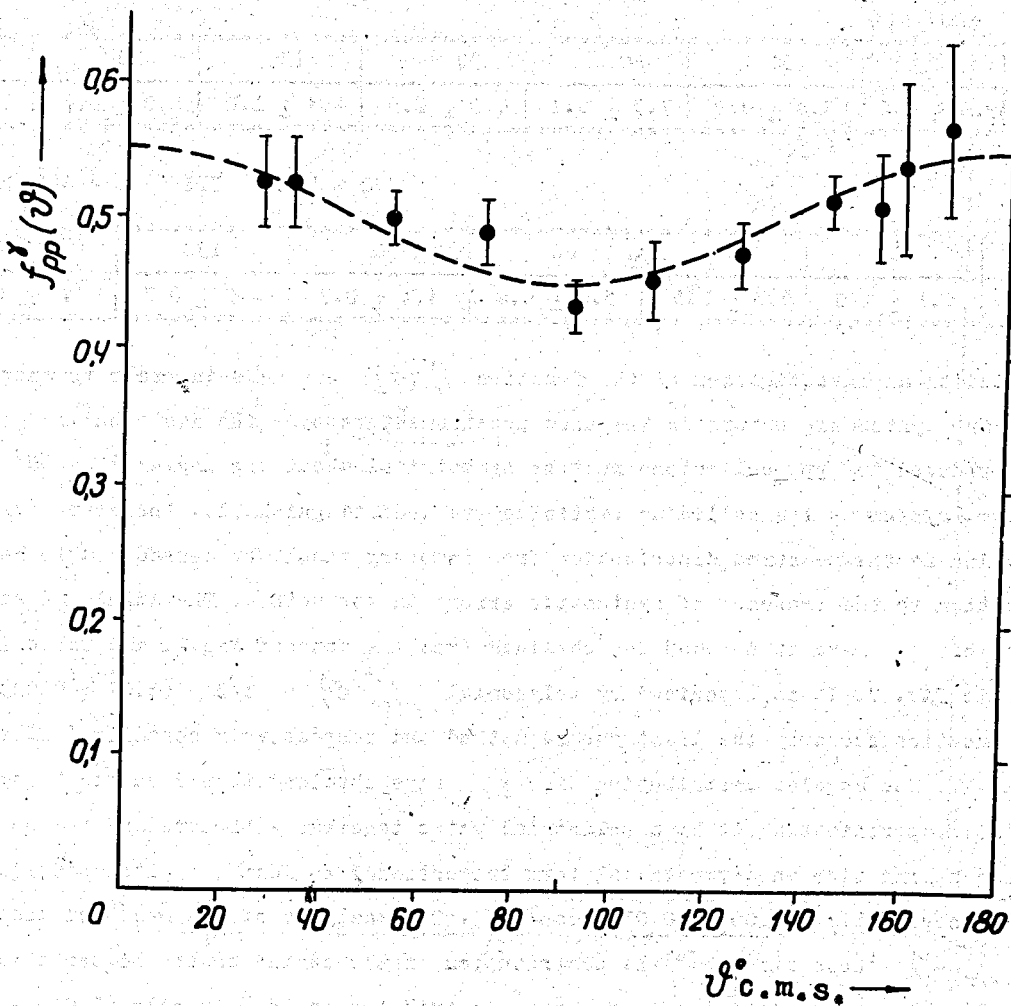


Fig. 7. Angular distribution of  $\gamma$  rays from the reaction (1) at  $E = 665$  Mev. The curve is plotted by the least square method (see the text).

To determine  $b_\gamma$  it is enough to find the ratio of  $\gamma$  ray yields at two different angles. Such measurements were made at energies lower than 660 Mev mainly with a liquid hydrogen target as the subtraction method provides high accuracy of determination of  $b_\gamma$  in the energy region  $E = 600$  Mev only, as is seen in Figs.7 and 8. Gamma-ray yields were measured at the angles  $\theta_1 = 55 - 60^\circ$  and  $\theta_2 = 120 - 125^\circ$ . The values  $\theta_1$  and  $\theta_2$  changed slightly with decreasing  $E$ . The angles  $\theta_1$  and  $\theta_2$  were taken as the supplement ones to avoid the difficulty connected with determination of the effective volume of the liquid hydrogen target. The choice of the above angles is due to the fact that measurements at these angles provide the best accuracy of determination of  $b_\gamma$  (if  $\theta_1 + \theta_2 = 180^\circ$ ). Finally, the indicated values  $\theta_1$  and  $\theta_2$  are convenient because in the c.m. system they correspond to the angles  $\varphi_1 = 90^\circ$  and  $\varphi_2 = 145^\circ$ , their differential cross sections being connected with the total cross section by a simple relation

$$\sigma^{\pi^0} = \pi \{ d\sigma^r(\varphi_1)/d\Omega + d\sigma^r(\varphi_2)/d\Omega \}, \quad (3)$$

which is valid with the arbitrary values of  $b_\gamma$ . At the energies  $E > 500$  Mev the measurements of  $b_\gamma$  were carried out both with the liquid hydrogen target and by the subtraction method. In the latter case  $\gamma$  ray yields were measured at several angles including angles  $\theta_1$  and  $\theta_2$ . The values  $b_\gamma$  found by these different methods are consistent within experimental errors. The values  $b_\gamma$  obtained are given in Table IV.

T a b l e I V

E Mev	665	630	590	560	517	485	440	400
$b_\gamma$	0050±0017	-002±004	006±005	002±003	005±006	001±004	-001±006	0015±0060

Reconstruction of  $\pi^0$  angular distribution

Angular distributions of  $\pi^0$  mesons can be reconstructed from those of  $\gamma$  rays. We shall show at first how this problem is solved in case of monoenergetic  $\pi^0$  mesons. Let  $\pi^0$  mesons have the velocity  $\beta$  and their angular distribution is described in the cm. system by the function  $V(\cos \vartheta, \varphi)$ . Angular distribution of  $\gamma$  rays from  $\pi^0$  meson decay  $F(\cos \vartheta, \varphi)$  is determined by the integral relation:

$$F(\cos \vartheta, \varphi) = (\xi^2 - 1) \int_0^{2\pi} \int_0^\pi V(\cos \vartheta_0, \varphi_0) [\xi - \cos \vartheta \cos \vartheta_0 - \sin \vartheta \sin \vartheta_0 \cos(\varphi - \varphi_0)]^{-2} d\cos \vartheta_0 d\varphi_0. \quad (4)$$

Here  $\xi = 1/\beta$ . We shall take a rather general case when angular distribution of  $\pi^0$  mesons does not depend upon the azimuthal angle  $\varphi$ . Then integrating (4) over  $\varphi_0$  obtain:

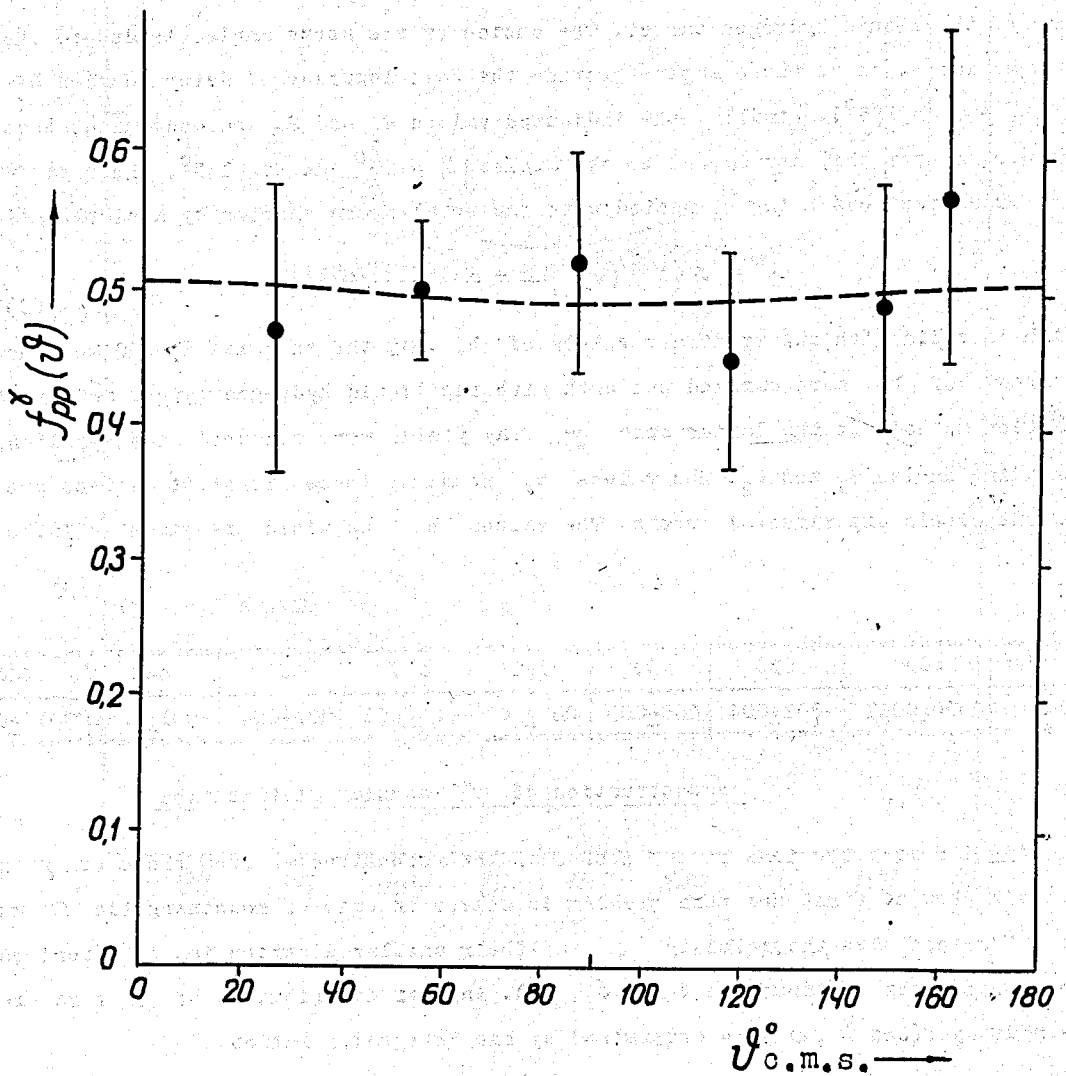


Fig. 8. Angular distribution of  $\gamma$  rays from the reaction (I) at  $E = 485$  Mev. The curve is plotted by the least square method and corresponds to the dependence  $f_{pp}^{\gamma}(\vartheta) \sim 1/3 + 0.02 \cos^2 \vartheta$ .

$$F(\cos\vartheta) = 1/2(\xi^2 - 1) \int_{-1}^{+1} V(\cos\vartheta_0) \mathcal{Y}(\cos\vartheta, \cos\vartheta_0) d\cos\vartheta_0. \quad (5)$$

The nucleus of the equation (5) is symmetrical:

$$\mathcal{Y}(\cos\vartheta, \cos\vartheta_0) = (\xi - \cos\vartheta \cos\vartheta_0) [(\cos\vartheta + \cos\vartheta_0)^2 - (\xi + 1)(2\cos\vartheta \cos\vartheta_0 - \xi + 1)]^{-1/2}.$$

The formula (5) permits to reconstruct the angular distribution of  $\pi^0$  mesons  $V(\cos\vartheta)$  if the angular distribution of  $\gamma$  rays is known. This task can be settled both by the method of approximating the equation (5) by the system of linear equations and by the method of eigenfunction expansion. (The eigenfunctions of equation (5) are the Legendre polynomials  $P_n(\cos\vartheta)$ ; this follows from (4) if using the "addition theorem" for Legendre polynomials). In the latter case representing  $F(\cos\vartheta)$  by a series  $\sum_n a_n P_n(\cos\vartheta)$  obtain

$$V(\cos\vartheta) = \sum_n \frac{a_n}{\alpha_n(\xi)} P_n(\cos\vartheta). \quad (6)$$

The eigenvalues  $\alpha_n(\xi)$  can be easily obtained making use of the Neiman formula for Legendre polynomials:

$$\alpha_n(\xi) = (\xi^2 - 1) Q'_n(\xi), \quad (7)$$

where  $Q'_n(\xi)$  is the derivative of the Legendre function of the second kind:

$$Q'_n(\xi) = P_n(\xi) \operatorname{Arctg}(1/\xi) - \sum_{k=0}^{n-1} \frac{2n-4k-1}{(2k+1)(n-k)} P_{n-2k-1}(\xi).$$

With the help of the above relations the problem of reconstructing the angular distribution of monoenergetic  $\pi^0$  mesons can be settled. This task becomes more complicated if  $\pi^0$  mesons are non-monoenergetic. In the most general case, when the function of  $\pi^0$  meson distribution  $\mathcal{U}(\cos\vartheta, \xi)$  cannot be separated into angular and energy variables, to reconstruct the distribution  $\mathcal{U}(\cos\vartheta, \xi)$  it is necessary to investigate the angular and energy distribution of  $\gamma$  rays. In case when the angular and energy variables can be separated, that is

$$\mathcal{U}(\cos\vartheta, \xi) = V(\cos\vartheta) R(\xi) \quad (8)$$

the function  $V(\cos\vartheta)$  can be reconstruct by using the mean eigenvalues  $\bar{\alpha}_n$  obtained as a result of averaging the function(7) over the spectrum  $R(\xi)$ . To make such an averaging in a general case it is necessary to know the spectrum  $R(\xi)$ . However, if the angular distribution of  $\gamma$  rays differs from isotropic one only slightly it is quite enough to have the rough information on the spectrum which can be found from kinematics of the reaction (I). This was used in the present work since, as is seen from Table IV, the measured angular distributions of  $\gamma$  rays are close

to isotropic. In finding the angular distribution of  $\pi^+$  mesons it was assumed that the distribution function can be represented in the form (8). As follows from (2) and (6) the angular distribution of  $\pi^+$  mesons have the form

$$f_{pp}^{\pi^+}(\vartheta) \sim \frac{1}{3} + b_{\pi^+} \cos^2 \vartheta. \quad (9)$$

The values of  $b_{\pi^+}$  at different proton energies are given in Table V.

Table V.

E Mev	665	630	590	560	517	485	440	400
$b_{\pi^+}$	0.10±0.03	-0.04±0.08	0.14±0.12	0.04±0.07	0.13±0.15	0.02±0.12	-0.03±0.16	0.07±0.25

Total cross sections of the reaction (I).

The differential cross section of  $\gamma$  ray production on carbon at the angle  $\theta = 33^\circ$  was measured at the proton energy  $E = 660$  Mev. Its value

$$d\sigma_{pc}^{\gamma}(33^\circ, 660 \text{ Mev})/d\Omega = (7.6 \pm 0.4) \times 10^{-27} \text{ cm}^2/\text{sterad}$$

is in a good agreement with a cross section measured on the internal beam of the accelerator<sup>II/</sup>. The integration of the obtained angular distribution of  $\gamma$  rays normalized to the above cross section gives the total cross section for the reaction (I):

$$\sigma_{pp}^{\pi^+}(660 \text{ Mev}) = (3.22 \pm 0.17) \times 10^{-27} \text{ cm}^2.$$

The result close to this was obtained in experiments where the liquid hydrogen target was used:

$$(3.4 \pm 0.4) \times 10^{-27} \text{ cm}^2.$$

The proton energy dependence of the total cross section for the reaction (I) was measured in the energy region 313 - 665 Mev. The yields of  $\gamma$  rays were measured at several angles including the "isotropic" angles<sup>II,18,21/</sup> ( $33^\circ$  and  $96^\circ$  in the lab. system at  $E = 660$  MeV) as well as at the angles  $\theta_1$  and  $\theta_2$ ; this made it possible to find easily the relation of the total cross sections at different proton energies. In determining the cross sections by the subtraction method the use was made of the energy dependencies of the cross sections for carbon measured at "isotropic" angles. One of them is given in Fig.9. The relative cross sections  $\sigma'_{pp}$  were determined by the subtraction method at the energies  $E \geq 400$  Mev (see Table VI).

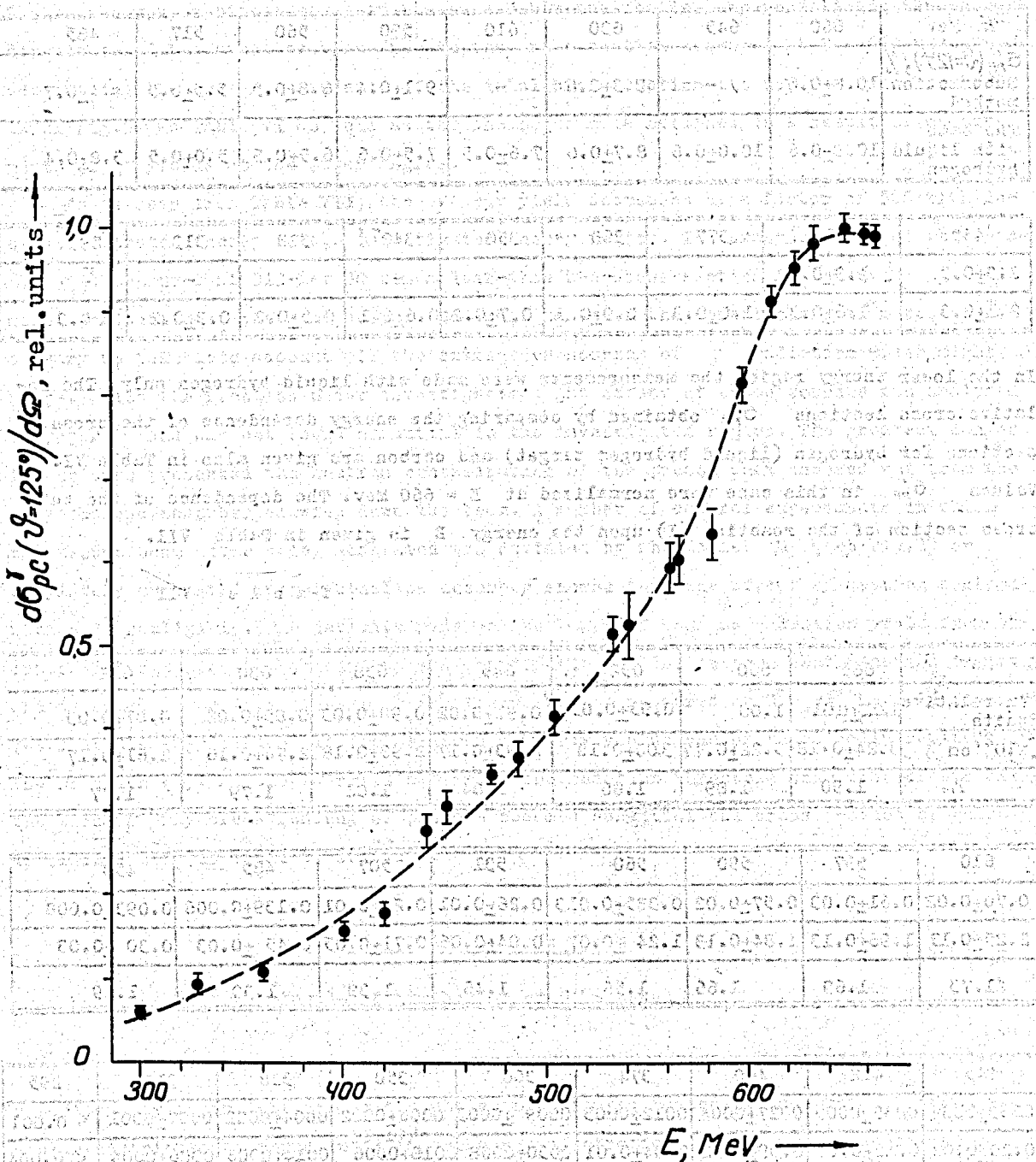


Fig. 9. Dependence of the cross section for  $\gamma$  ray production on carbon upon the proton energy  $E$ .

Table VI.

E Mev	660	645	630	610	590	560	517	485
$\sigma'_{pp}(\theta=125^\circ), \%$ Subtraction method	10.8±0.6	-	9.3±0.6	-	9.1±0.4	6.8±0.5	5.5±0.5	4.4±0.7
The same with liquid hydrogen	10.8±0.6	10.0±0.6	8.7±0.6	7.6±0.5	7.5±0.6	6.5±0.5	5.0±0.5	3.8±0.4

445	400	377	360	350	3407/	328	313	295
2.9±0.5	1.3±0.4	-	-	-	-	-	-	-
2.1±0.3	1.6±0.3	1.0±0.3	0.9±0.3	0.7±0.2	0.6±0.1	0.5±0.2	0.3±0.2	< 0.3

In the lower energy region the measurements were made with liquid hydrogen only. The relative cross sections  $\sigma'_{pp}$  obtained by comparing the energy dependence of the cross sections for hydrogen (liquid hydrogen target) and carbon are given also in Table VI. Values  $\sigma'_{pp}$  in this case were normalized at E = 660 Mev. The dependence of the total cross section of the reaction (I) upon the energy E is given in Table VII.

Table VII.

E Mev	665	660	652	645	638	630	622
$\sigma_{pp}$ in relative units	1.01±0.01	1.00	0.93±0.03	0.91±0.02	0.90±0.03	0.85±0.02	0.81±0.03
$\sigma_{pp} \times 10^{27} \text{ cm}^{-2}$	3.24±0.18	3.22±0.17	3.00±0.18	2.93±0.17	2.90±0.18	2.74±0.16	2.61±0.17
$\eta_m$	1.90	1.89	1.86	1.84	1.82	1.79	1.77

610	597	590	560	531	507	485	458
0.70±0.02	0.61±0.03	0.57±0.02	0.385±0.013	0.26±0.01	0.22±0.01	0.139±0.006	0.093±0.008
2.25±0.13	1.96±0.13	1.84±0.13	1.24±0.07	0.84±0.06	0.71±0.05	0.45±0.03	0.30±0.03
1.73	1.69	1.66	1.56	1.46	1.38	1.30	1.19

445	412	400	374	360	350	328	313	295
0.063±0.004	0.039±0.005	0.027±0.004	0.012±0.003	0.009±0.003	0.006±0.002	0.004±0.002	0.002±0.001	< 0.001
0.20±0.02	0.12±0.02	0.09±0.02	0.04±0.01	0.030±0.008	0.018±0.006	0.014±0.006	0.006±0.004	< 0.004
1.14	1.00	0.95	0.83	0.75	0.70	0.58	0.48	0.32



The total cross sections given in the same Table are obtained by normalizing the energy dependence of the cross section  $\sigma_{pp}^{\pi}$  to the cross section measured at  $E = 660$  Mev. In determining the energy dependence of the total cross section the use was made of the data of Fig.9 and Table VI as well as the analogous data obtained as a result of measurements of  $\gamma$  yields at the other angles.

As is seen from Table VII, the  $\gamma$  ray yield decreases by a factor of 500 with decreasing proton energy in the investigated energy region. The cross section of the reaction (I) measured at 313 Mev 30 times less than the cross section for charged  $\pi$  meson production at the same energy. So small value of the effect observed makes it necessary to take into account all the extraneous sources of  $\gamma$  radiation which might compete with the reaction under investigation. The effect of these sources was analysed in paper<sup>17/</sup> and was not found essential in the investigated region. The greatest danger in our case presented the neutron contamination of the proton beam knocked out from the polyethelene absorber slowing down the beam. A number of control experiments in which the proton beam after being moderated was deviated by the magnet M (see Fig.2) or completely moderated in polyethelene absorber showed that the effect of neutron contamination is negligible. The estimate made on the bases of the known neutron yield from the internal target<sup>22/</sup> also shows that the contribution of the neutron contamination is small and is equal to no more than 3% of the cross section measured at  $E = 313$  Mev. In the investigated energy region all the measured  $\gamma$  ray yields can be practically related to the reaction (I). At the energies closer to the reaction threshold than that of our case, the hard  $\gamma$  ray bremsstrahlung of protons becomes essential the cross section of which according to<sup>23/</sup> is equal to  $10^{-30}$  cm<sup>2</sup>.

#### 4. Discussion

##### Angular distribution of $\pi^+$ mesons

The characteristic feature of the angular distributions of  $\pi^+$  mesons obtained in our experiment is their isotropy in the whole investigated region of the proton energy. The angular distributions found in<sup>11,17/</sup> are more anisotropic at small proton energies, as is seen in Fig. 10. In this figure the energy dependence of  $S=I/I + b_{\pi^+}$  is given, which is the fraction of mesons distributed isotropically in the case if the angular

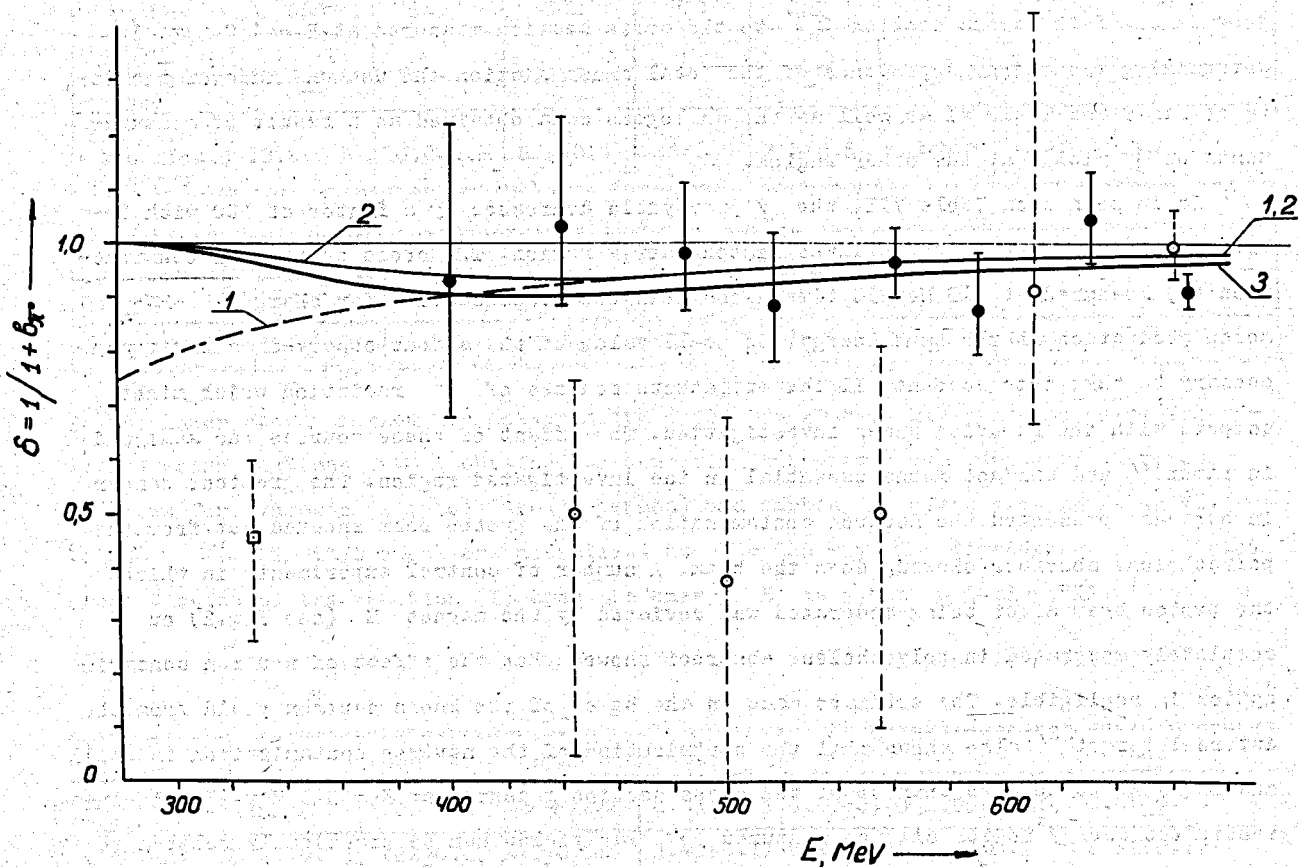


Fig. 10. Angular distribution of  $\pi^0$  mesons in the reaction (I) /function  $\delta(E)$ /.  
 $b_{\pi^0}$  is the coefficient in distribution (8) (see the text).

$\bar{\delta}$  - the results of the present work.

$\bar{\delta}^{\text{II}}$  - the data of II/.

$\bar{\delta}^{\text{I7}}$  - the data of I7/.

The curves are calculated: I - on the assumption of (10) without taking into account non-resonant Ss-transition. 2 - the same as I but the account was taken of Ss-transition. 3 - on the assumption of (II) with account taken of Ss-transition.

distribution has the form(9) and  $b_{\pi} \geq 0$ . The value  $S$  at  $E=329$  Mev was determined the detector with high energy threshold<sup>17/</sup> and thus, it depends essentially upon the validity of the theoretical assumption made with respect to the  $\pi^0$  meson distribution function. The present phenomenological theories<sup>1,9,13/</sup> differ in their conclusions on the function of  $\pi^0$  meson distribution in the reaction (I). Experimentally determined values  $S$  are compared in Fig. 10. with the dependence  $S(E)$  calculated by Mandelshtam (private communication)\* on the basis of the theory<sup>13/</sup>. The curve (I) in this figure is calculated taking account of the resonant transitions. At high energies the value  $S$  turns out to be close to unity. According to<sup>13/</sup> this is a consequence of predomination of the P state production over the S one which is practically suppressed as a result of interference. While approaching to the reaction threshold the anisotropy of the angular distribution of  $\pi^0$  mesons produced in the resonant transitions increases. However, the contribution of the resonant transitions in this energy region is rather small. Non-resonant Ss-transition characterized by the isotropic angular distribution  $\pi^0$  mesons is predominant here. Therefore the dependence  $S(E)$  calculated taking account of nonresonant Ss transition turns out to be close to unity in all the investigated energy region; this is in a good agreement with the results of the present paper.

The values  $S$  given in Fig. 10 were determined here from the experimental data on the values  $b_{\pi}$  with the assumption that the angular and energy fraction of  $\pi^0$  meson distribution are independent (see the formula (8)). The Mandelshtam theory, however, predicts that the anisotropy of angular distribution of  $\pi^0$  mesons is the less, the lower is their energy, and near the lower boundary of the spectra the coefficient  $b_{\pi}$  becomes even negative (contrary to<sup>1,9/</sup>). Therefore, if the values  $S$  are calculated from the data of Table IV on the basis of the spectra taken from Mandelshtam theory, they are situated a little nearer to unity than it is shown in Fig. 10.

---

\*) We take the opportunity to thank Dr.S. Mandelshtam who has kindly sent us the results of the number of his unpublished calculations.

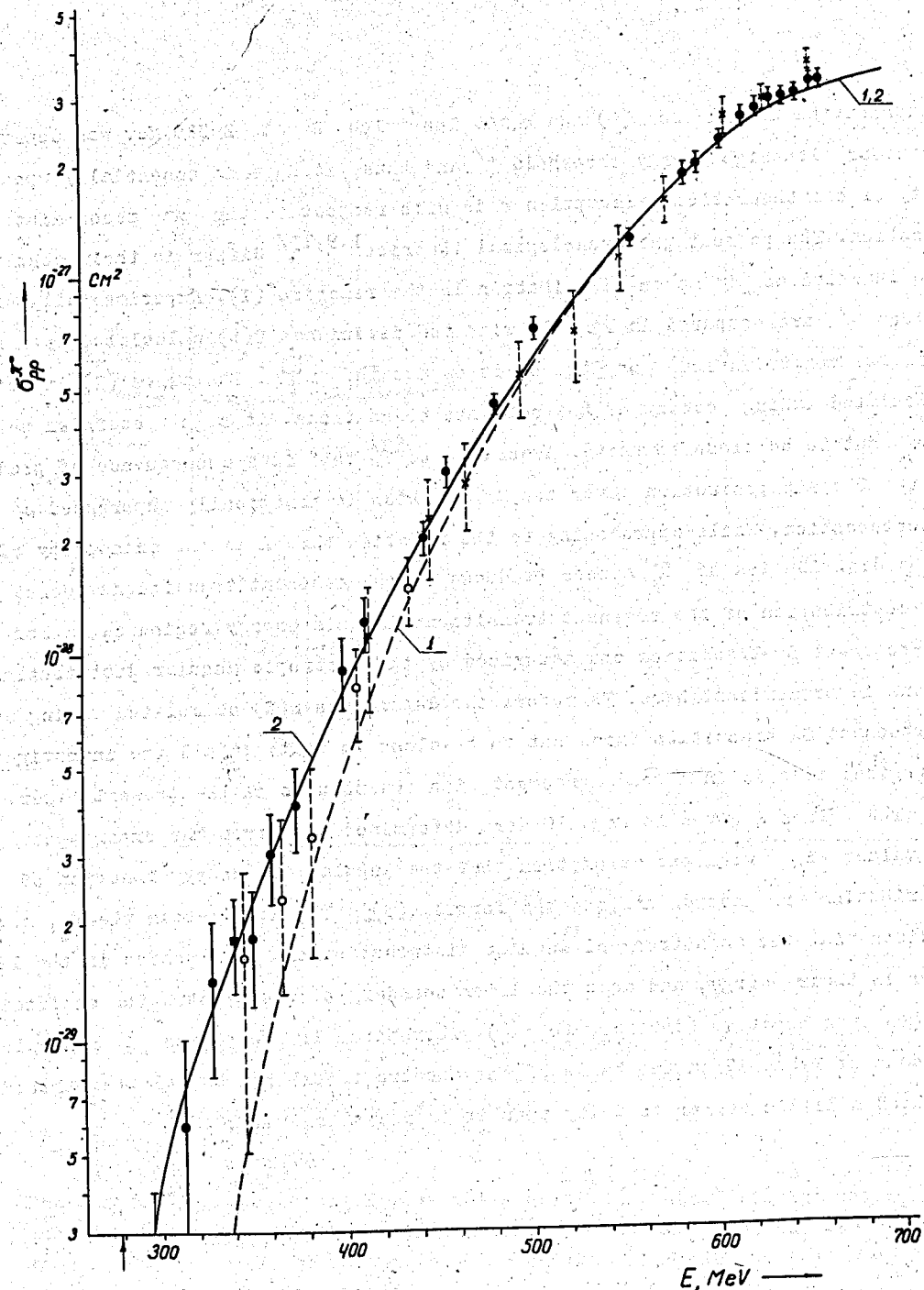


Fig. II.

The total cross sections of the reaction (I)

$\bar{\sigma}$  - the results of the present work,

$\bar{\sigma}$  - the results of the present work and (7),

$\bar{\sigma}$  - the results of <sup>11</sup>/,  $\bar{\sigma}$  - the results of <sup>12</sup>/.

The arrow indicates the reaction threshold. 1.-The resonant curve calculated in <sup>13</sup>/. 2.-The curve taking into account the non-resonant Ss transition the contribution of which to the total cross section is equal to  $0.032 \eta_m^2 10^{-27} \text{ cm}^2$ .

Energy dependence of the reaction (I) cross section

The measured in the present investigation total cross sections are given in Fig. II. Here the cross section is given in determining of which the present paper data were used on the cross section value for carbon as well as Mather and Martinelli's data on the relative cross section  $\sigma_{pp}'$  (see Table VI). The total cross section  $\sigma_{pp}^{\pi^+}(340\text{Mev}) = (0.018 \pm 0.005) \times 10^{-27} \text{cm}^2$  is twice as large as the value of the cross section  $(0.010 \pm 0.003) \times 10^{-27} \text{cm}^2$  previously found from the data<sup>7,8/</sup> and usually used in earlier investigations. The reason of this difference is in the divergence of cross sections for carbon measured in the present paper:  $(3.0 \pm 0.4) \times 10^{-27} \text{cm}^2$  and in<sup>8/</sup> -  $(1.7 \pm 0.4) \times 10^{-27} \text{cm}^2$ . It should be noted that the cross section for charged  $\pi$  meson production on carbon at this energy is equal<sup>24/</sup> to  $(7.5 \pm 1.0) \times 10^{-27} \text{cm}^2$ . From this follows that  $\sigma_{pc}^{\pi^+} = (3.7 \pm 0.5) \times 10^{-27} \text{cm}^2$  if using the relation  $\frac{1}{2}(\sigma_{pc}^{\pi^+} + \sigma_{pc}^{\pi^-}) = \sigma_{pc}^{\pi^0}$  which follows from the hypothesis of charge independence of nuclear forces and is rather accurately fulfilled in the experiment<sup>25/</sup>.

As is seen from Fig. II the measured cross sections are in agreement (within experimental errors) with values found earlier<sup>11/</sup>. The cross sections measured in Carnegie<sup>12/</sup> are placed somewhat below than those obtained in the present investigation; this can be explained by the increase in<sup>12/</sup> of  $\gamma$ -telescope efficiency. The calculated in this paper efficiency at high energies of  $\gamma$  rays exceeds its maximum possible value equal to  $1 - \exp(-\mu d)$ . Here  $\mu$  is the coefficient of  $\gamma$  absorption in the converter matter,  $d$  is the converter thickness.

The obtained total cross sections are compared in Fig. II with the theoretical resonance curve of Mandelshtam. This comparison shows that the behaviour of the reaction cross section in the energy region near 600 Mev can be accurately described by the theory taking into account only resonant transitions. In the energy region below 500 Mev the marked difference between the measured cross sections and the resonant curve begins to appear; this can be explained<sup>13/</sup> by the increasing of the role of non-resonant Ss-transition which is essential near the reaction threshold. We have found the contribution to the total cross section corresponding to this transition by comparing the measured cross sections with a resonant curve. It turned out to be

$$\sigma_{Ss} = (0.032 \pm 0.007) \varrho_m^2 \cdot 10^{-27} \text{cm}^2.$$

Taking into account the contribution of the resonant transitions<sup>13/</sup> the cross section of the reaction (I) near the threshold at energies below 400 Mev can be represented in the form

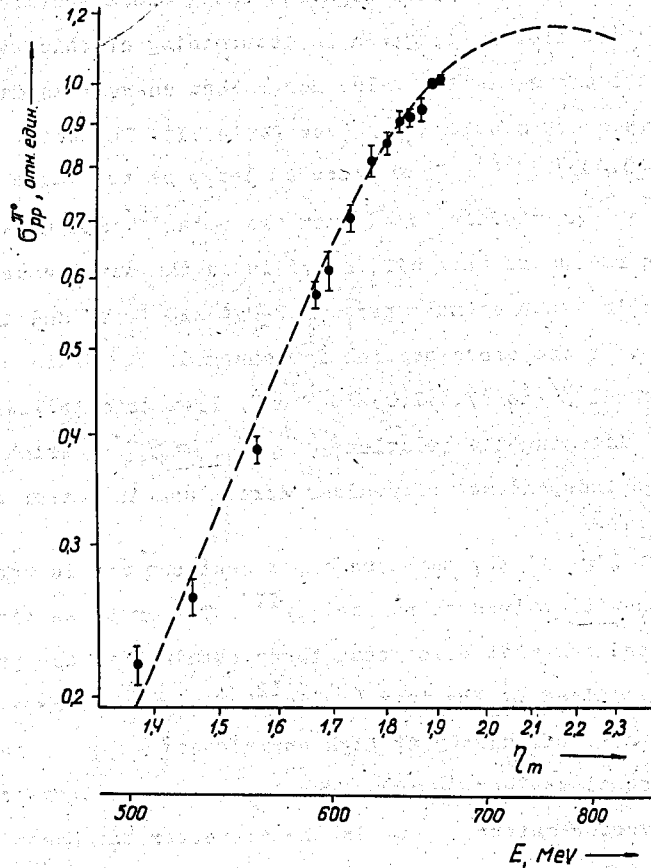


Fig. 12. Dependence of the reaction (I) cross section upon the momentum  $q_m$  in the region of maximum. Experimental data and the theoretical curve taken from<sup>13/</sup> are normalised at  $E = 660$  Mev. The errors indicated in this figure correspond to those of the relative measurements of the energy dependence of the cross section and therefore they are less than the errors of Fig. II showing the errors of the absolute measurements of the cross sections.

$$\sigma_{pp}^{\pi^0} = (0.032\eta_m^2 + 0.040\eta_m^6 + 0.047\eta_m^8) \times 10^{-27} \text{ cm}^2.$$

Here the first term is due to non-resonant Ss-transition, the second - to "displaced" Ss- and Sd-transitions and the last - to Pp-transition. Ps-transition characterized also by the dependence  $\eta_m^6$  is not considered essential in the theory of Mandelshtam. In the energy region 450 - 600 Mev the cross section of the reaction under investigation increases with constant velocity changing as  $\eta_m^{3.7}$ . In the higher energy region the cross section growth is reduced in agreement with the theory of Mandelshtam. (see Fig.12).

The comparison of cross sections for the production of neutral and charged  $\pi$  mesons in proton-proton collisions.

Using the results of the present investigation and the data<sup>26/</sup> one can obtain the information on the value of the ratio  $\pi^0/\pi^+ = \sigma_{pp}^{\pi^0} / \sigma_{pp,\rho n}^{\pi^+}$  where  $\sigma_{pp,\rho n}^{\pi^+}$  is the cross section of the reaction  $p + p \rightarrow p + n + \pi^+$  in the final state of which nucleons are not bound (see Fig. 13). At the energy 660 Mev this ratio is equal to

$$\pi^0/\pi^+ = 0.294 \pm 0.015 .$$

The ratio  $\pi^0/\pi^+$  was calculated by Peaslee<sup>27/</sup> for the case when all the transitions are made through the resonant state ( $T=3/2, J=3/2$ ) and was found to be 1/5. The interfeerention of the nucleon states and the difference in  $\pi$  meson masses taken into account have changed this value and brought it nearer to the experimental data<sup>13/</sup>. The curves given in Fig. 13 were calculated by Mandelshtam (private communication) by taking account of Ss-transition. The lower curve is calculated on the assumption<sup>13/</sup> that three parameters describing P state production in states of the total angular momentum  $J=2,1,0$  are equal to

$$|b_{2a}| = |b_{1a}| = |b_{0I}| = |b_a| , \tag{10}$$

where  $b_a$  is one of two free parameters of P state production in the resonant theory. This assumption was made somewhat arbitrary. As is indicated in the private communication of Mandelshtam the following assumption is more correct

$$|b_{2a}|^2 = 2|b_{1a}|^2 = 2|b_{0I}|^2 . \tag{II}$$

That is,  $\pi^0$  meson production in  $J=2$  state is more probable than  $J=1$  and  $J=0$ . In the latter case the better agreement of calculated ratio  $\pi^0/\pi^+$  with experimental data is observed (see Fig. 13). The other circumstance in favour of the relation (II) (as is pointed out in the private communication of G. Brown) is the small value

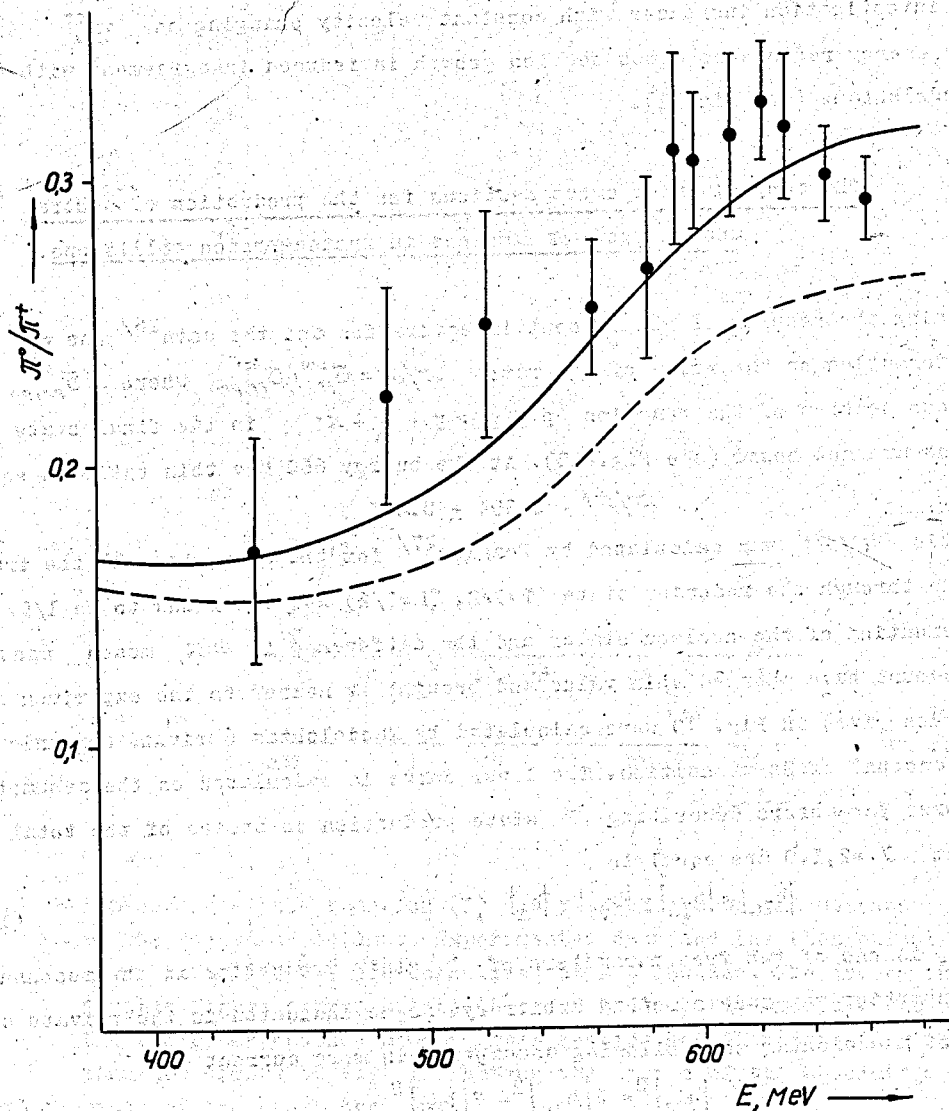


Fig. 13. The ratio of the cross sections for  $\pi^0$  and  $\pi^+$  meson production by protons of different energies. The solid curve is calculated on the assumption of the equality (11), the dashed curve of the equality (10).



of the radius of proton interaction in  ${}^3P_2$  state in comparison with  ${}^3P_1$  and  ${}^3P_0$ . Due to this the meson production in  $J=2$  state is less inhibited than with  $J=1$  and  $J=0$ .

Thus, the value  $\pi^0/\pi^+$  turns out to be sensitive to the relation of different P state production parameters. The other characteristics of the reaction (I) are less sensitive to the change of parameter relation. So, the angular distribution of  $\pi^0$  mesons calculated for the cases (10) and (II) practically does not differ; this is seen in Fig. 10.

In the energy region  $E \gtrsim 600$  Mev the measured energy dependence of the ratio  $\pi^0/\pi^+$  is not monotonic. The reason of this is the different behaviour of the measured cross sections  $\sigma_{pp}^{\pi^0}$  and  $\sigma_{pp,pn}^{\pi^+}$ : while the increase of the cross section is reduced at  $E \gtrsim 600$  Mev, the cross section  $\sigma_{pp,pn}^{\pi^+}$  goes on increasing as fast as it was in the low energy region.

### 5. C o n c l u s i o n

The comparison of the experimental data with Mandelshtam theory made in the present paper shows that the accuracy with which this theory describes the main properties of the process of  $\pi^0$  meson production by protons at  $E < 700$  Mev is very large. In connection with this the further systematic investigation of this reaction in the region of higher energies 700 - 1000 Mev where (according to the theory) its cross section passes through the maximum is of great interest. The data<sup>28/</sup> obtained up till now in this energy region disagree; this does not permit to use them for their comparison with the theory.

In conclusion we wish to thank L.I. Lapidus, S. Mandelshtam, L.M. Soroko and A.A. Tyapkin for discussion the results of the present investigation. We are thankful to E.L. Grijorjev, M.M. Kulyukin, N.A. Mitin and O.V. Savchenko for their help in performing the measurements.

References

1. A. Rosenfeld, Phys. Rev. 96, 139, 1954.
2. R. Hales, R. Hildebrand, N. Knable, B. Moyer, Phys. Rev. 85, 37, 1952.
3. J. Marshall, L. Marshall, V. Nedzel, S. Warshaw, Phys. Rev. 88, 632, 1952.
4. B. Pontecorvo, G. Selivanov, V. Zhukov, The report of the Institute for Nuclear problems of the USSR Acad. of Sci., 1952, p. 81.
5. M. Kozodaev, A. Tyapkin, Yu. Bayukov, A. Markov, Yu. Prokoshkin, Izv. Acad. Nauk SSSR, ser. fiz. 19, 589, 1955.
6. L. Soroko, JETP 30, 296, 1956.
7. J. Mather, E. Martinelli, Phys. Rev. 92, 780, 1953.
8. W. Crandall, B. Moyer, Phys. Rev. 92, 749, 1953.
9. M. Gell-Mann, K. Watson, Annual Rev. Nucl. Science 4, 219, 1954.
10. A. Tyapkin, M. Kozodaev, Yu. Prokoshkin, Dokl. Acad. Nauk 100, 689, 1955.
11. Yu. Prokoshkin, A. Tyapkin, JETP, 32, 750, 1957.
12. R. Stallwood, R. Sutton, T. Fields, J. Fox, J. Kane, Phys. Rev. 101, 1716, 1958.
13. S. Mandelstam, Proc. Roy. Soc. A. 244, 491, 1958.
14. B. Balashov, V. Zhukov, B. Pontecorvo, G. Selivanov, (see 15, p. 393).
15. Yu. Prokoshkin, Proc. CERN Symposium, 2, 385, 1956.
16. Yu. Bayukov, A. Tyapkin, JETP, 32, 953, 1957.
17. B. Moyer, R. Squire, Phys. Rev. 107, 283, 1957.
18. Yu. Prokoshkin, JETP, 31, 732, 1956.
19. I. Vasilevskiy, Yu. Prokoshkin, Atomnaya Energiya (in press).
20. Yu. Bayukov, M. Kozodaev, A. Tyapkin, JETP, 32, 667, 1957.
21. A. Tyapkin, JETP, 30, 1150, 1956.
22. V. Dzhelepov, B. Pontecorvo, Atomn. Energ. 3; N II, 413, 1957.
23. A. Ashkin, R. Marshak, Phys. Rev. 76, 58, 1949; R. Bjorklund, W. Carandall, B. Moyer, H. York, Phys. Rev. 77, 213, 1950.
24. C. Richman, H. Weissbluth, H. Wilcox, Phys. Rev. 85, 161, 1952;  
S. Passman, M. Block, W. Havens, Phys. Rev. 88, 1247, 1952; S. Leonard, Phys. Rev. 93, 1380, 1954; W. Dudziak, Phys. Rev. 95, 866, 1954.
25. A. Meshkovskiy, Yu. Pligin, Ya. Shalamov, V. Shebanov, JETP, 32, 1328, 1957.
26. B. Neganov, O. Savchenko, JETP, 32, 1265, 1956; V. Dzhelepov, V. Moskalev, S. Medved, Dokl. Acad. Nauk, 104, 380, 1955, The report at the conference on high energy physics, Moscow, 1956; M. Mescheryakov, B. Neganov Dokl. Acad. Nauk, 100, 677, 1955; T. Fields, J. Kane, R. Stallwood, R. Sutton, Phys. Rev. 109, 1713, 1958.
27. D. Peaslee, Phys. Rev. 95, 1580, 1954.
28. J. Huges, P. March, P. Muirhead, W. Look, Proc. CERN Symposium, 2, 344, 1956.  
T. Morrison, E. Fowler, J. Garrison, Phys. Rev. 103, 1472, 1956.

Received by Publishing Department in December 22, 1958.